ISJ 8: 98-108, 2011 ISSN 1824-307X

RESEARCH REPORT

Alteration of mitochondrial membrane potential (ΔΨm) and phosphatidylserine translocation as early indicators of heavy metal-induced apoptosis in the earthworm *Eisenia hortensis*

FM Bearoff, SL Fuller-Espie

Science Department, Cabrini College, 610 King of Prussia Road, Radnor, Pennsylvania 19087-3698, USA

Accepted June 3, 2011

Abstract

The effects of the heavy metals cadmium and copper (50-500 μM) on the apoptotic events involving changes in mitochondrial membrane potential (ΔΨm) and phosphatidylserine (PS) translocation were investigated in the immune cells (celomocytes) of the earthworm *Eisenia hortensis.* Using the fluorescent probe JC-1*,* loss of membrane potential due to depolarization was detected in a greater proportion of cases when induced by cadmium compared to copper (58.7 % vs. 37 %) and at a lower concentration (50 μM vs. 125μM). With the use of the general caspase inhibitor Z-VAD-fmk, PS translocation detected by annexin V-FITC was found to be caspase-dependent when induced by cadmium at 125-250 μM but not at 50 μM or 500 μM; a high proportion of earthworms (60 %) exhibited inhibitory effects. Additionally, the collapse in membrane potential and PS translocation were found to strongly correlate (r > 0.5) in 89 % of cases when induced by cadmium and copper. Thus, heavy metals appear to induce death in celomocytes of *E. hortensis* through apoptosis by means of caspase dependent pathways.

Key Words: cadmium and copper; JC-1; annexin V-FITC; mitochondrial membrane depolarization; phosphatidylserine translocation; caspases

Introduction

Programmed cell death (PCD) is a universal cellular process in which the induction of a tightly regulated signal cascade ultimately leads to the destruction of the cell. It serves multiple roles such as facilitating death of the mother cell during spore formation in the bacterium *Bacillus subtilis*, removal of tissue during fetal development, and elimination of infected tissues in both plants and animals (Haanen and Vermes, 1996; Lewis, 2000; Collazo and Chacón, 2006; Kinchen, 2010; Harrison *et al*., 2011). In multicellular organisms, apoptosis is the mode of PCD characterized by many morphological changes such as membrane blebbing, nuclear DNA fragmentation, loss of mitochondrial membrane potential (ΔΨm), and phosphatidylserine (PS) translocation across the plasma membrane (Ly *et al*., 2003; Kiss, 2010). Many of these apoptotic events are initiated through caspases which are cysteine proteases that initiate signal cascades by cleaving at aspartic acid residues (Shimizu and Pommier, 1997). These signal cascades can be initiated in times of cellular stress by many factors such reactive oxygen species (ROS) generation, exogenous H_2O_2 exposure, cytokine stimulation, and exposure to environmental pollutants such as heavy metals and cytotoxic organic compounds like camptothecin (Shimizu and Pommier, 1997; Blanco *et al*., 2005; Belyaeva *et al*., 2008; Kim *et al*., 2008; Fuller-Espie *et al*., 2010).

Heavy metals such as cadmium and copper are increasingly becoming an environmental concern due to the improper disposal of electronic devices such as cell phones and batteries in which they are used. Toxicity associated with accumulation of cadmium and copper in soil has been shown in both plant and earthworm (EW) models leading to decreased root growth, mortality, and DNA damage due to increased production of 8-oxoguanine (An, 2004; Arnold *et al*., 2004; Hirano and Tamae, 2010). EWs are well suited for assessing soil quality since they bioaccumulate these metals and have relativity long life spans at an average of 4.25 years (Morgan and Morgan, 1988; Mulder *et al*., 2007; Hirano and Tamae, 2010).

Corresponding author:
Sheryl L. Fuller-Espie
Science Department, Cabrini College
610 King of Prussia Road, Radnor, Pennsylvania 19087-3698, USA
E-mail: sfuller-espie@cabrini.edu

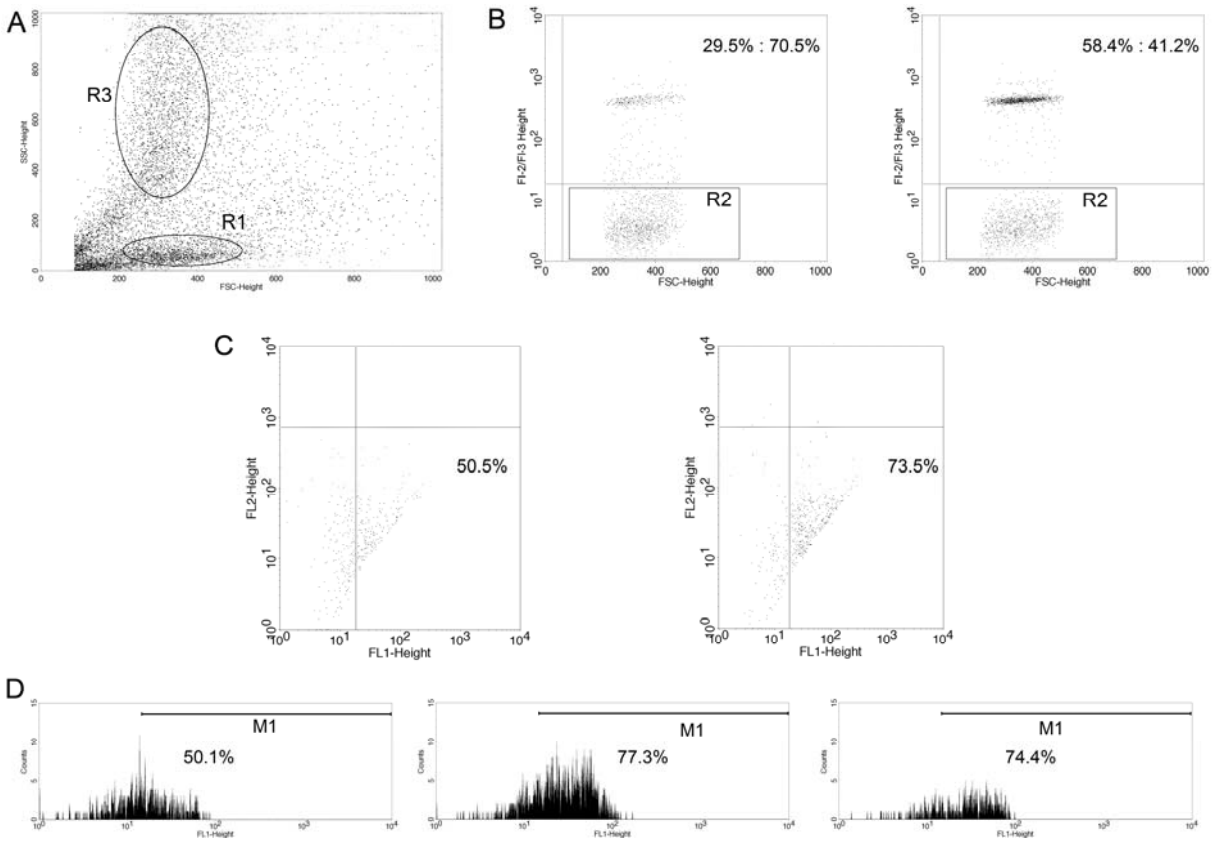

Fig. 1 Representative flow cytometry profile for all assays. (A) shows a typical celomocyte profile of FSC (size) (abscissa) versus SSC (granularity) (ordinate) of extruded EW celomocytes where R1 = hyaline and granular amebocytes and R3 = eleocytes. (B) shows FSC (abscissa) versus FL-2/3 fluorescence (ordinate) of R1 gated celomocytes. R2 depicts PI-negative (Fl-2 negative) or 7-AAD negative (FL-3 negative) viable amebocyte populations. Left dot plot indicates untreated celomocytes while right dot plot indicates cadmium-treated celomocytes. Percentages in upper right and lower right quadrants are shown corresponding to dead and alive celomocytes, respectively. (C) depicts FL-1 (abscissa) versus FL-2 (ordinate) of amebocytes gated on R1 and R2 and stained with 7-AAD plus JC-1 in ΔΨm assays. Therefore, gated events represent only viable amebocytes that have not taken up 7-AAD. Events in lower right quadrant set at the median FL-1 fluorescence value of the untreated control were counted as positive. Percentages in lower right quadrant are indicated for untreated (left dot plot) and cadmium-treated (right dot plot) celomocytes. (D) depicts FL-1 (abscissa) versus cell number (ordinate) of amebocytes gated on R1 and R2. Events in the M1 marker set at the median FL-1 fluorescence value of the untreated control were counted as positive for ΔΨm (JC-1) and PS (annexin V FITC) assays. Shown are ΔΨm results for untreated (left), valinomycin-treated (middle) and cadmium-treated (right) celomocytes. FSC = forward scatter; SSC = side scatter; FL-1 = relative fluorescence intensity of FITC and monomeric JC-1, FL-2 = relative fluorescence intensity of PI (PS assays) or J-aggregates (ΔΨm assays), FL-3 = relative fluorescence intensity of 7-AAD.

The primary goal of this *in vitro* study was to investigate the effects of the heavy metals cadmium and copper on the early apoptotic events of involving ΔΨm and PS translocation in the immune cells (celomocytes) of the EW *Eisenia hortensis (*also known as the European nightcrawler*)*. Mitochondrial membrane potential (ΔΨm) is the product of stored energy for the mitochondrial respiratory chain maintained by a balance of ions such as sodium and potassium within the mitochondrion. This potential difference normally exists at -180 to -200 mV and is necessary for transport of precursor proteins into the mitochondrion (Martin *et al*., 1991; Cossarizza *et al*., 1995). During early apoptosis the mitochondrial membrane becomes depolarized leading to increased permeabilization and the release of mitochondrial contents which, in addition to cytochrome c, contains a second mitochondria-derived activator of caspases (SMACs) that initiate apoptosis through the deactivation of inhibitor of apoptosis (IAP) proteins (Fesik and Shi, 2001). It has been shown that mitochondria are target organelles for heavy metals and can induce the apoptosis signal cascade (Belyaeva *et al*., 2008). PS translocation from the inner to outer leaflet of the cellular membrane is also associated with early apoptosis

Table 1 Loss of ΔΨm in response to cadmium and copper exposure

$\Delta\Psi_m$	Cd50	Cd125	Cd250	Cd500	Cu50	Cu125	Cu250	Cu500
EW-J1	-	T	T*	-	-	T	T	-
EW-J2	-	T	T	-	-	T	T	-
EW-J3	-	T*	T*	T*	-	T*	T*	T*
EW-J4	-	T	T	T*	-	T	T	T
EW-J5	-	T	T*	T*	-	T	T	T
EW-J6	-	-	-	T*	-	-	-	T
EW-J7	-	-	-	T	-	-	-	T
EW-J8	-	-	-	T	-	-	-	T
EW-J9	-	-	-	T*	-	-	-	T*
EW-J10	-	-	-	T	-	-	-	T
EW-J11	-	-	-	T*	-	-	-	T
EW-J12	-	-	-	T*	-	-	-	T
EW-J13	-	-	-	T*	-	-	-	T
EW-J14	-	-	-	T	-	-	-	T
EW-J15	-	-	-	T	-	-	-	T
EW-J16	-	-	-	T*	-	-	-	T*
EW-J17	-	-	-	T*	-	-	-	T
EW-J18	-	-	-	T*	-	-	-	T*
EW-J19	-	-	-	T	-	-	-	T
EW-J20	-	-	-	T*	-	-	-	T
% Response of EW-J1-20	**-** **(0/0)**	**20%** **(1/5)**	**60%** **(3/5)**	**66.7%** **(12/18)**	**-** **(0/0)**	**20%** **(1/5)**	**20%** **(1/5)**	**22.2%** **(4/18)**
EW-JA1	-	-	T*	T*	-	-	T*	T*
EW-JA2	-	-	T	T	-	-	T*	T*
EW-JA3	-	-	T	T*	-	-	T*	T*
EW-JA4	T*	-	-	T*	T	-	-	T*
EW-JA5	T	-	-	T*	T	-	-	T*
EW-JA6	T	-	-	T*	T	-	-	T*
EW-JA7	T*	-	-	T*	T	-	-	T*
EW-JA8	T	-	-	T*	T	-	-	T
EW-JA9	T*	-	-	T	T	-	-	T*
% Response of EW-JA1-9	**50%** **(3/6)**	**-** **(0/0)**	**33%** **(1/3)**	**77.8%** **(7/9)**	**0%** **(0/6)**	**-** **(0/0)**	**100%** **(3/3)**	**88.9%** **(8/9)**
% Response	**50%** **(3/6)**	**20%** **(1/5)**	**50%** **(4/8)**	**70.4%** **(19/27)**	**0%** **(0/6)**	**20%** **(1/5)**	**50%** **(4/8)**	**44.4%** **(12/27)**
Total Response	**58.7%** **(27/46)**				**37%** **(17/46)**			

Shown is a summary of all EWs treated with cadmium and copper at 50 μM, 125 μM, 250 μM, and 500 μM. Statistically significant increases ($p \leq 0.05$) were greater for cadmium at all concentrations compared to copper with total responses of 58.7 % and 37 % respectively. - = not tested, T = tested, T* = tested and statistically significant.

and is brought about by the oxidation of these phospholipids with caspase-3 involvement (Kagan *et al*., 2000; Mandal *et al*., 2002). The externalization of PS serves as a signal for engulfment of apoptotic cells by phagocytes (Fadeel and Xue, 2009).

EW celomocytes reside in the celomic cavity and consist of three distinct subpopulations which are most likely derived from a common progenitor cell (prohemocyte): hyaline amebocytes (large celomocytes), granular amebocytes (small celomocytes), and chloragocytes (eleocytes) (Hartenstein, 2006). Functionally, the hyaline amebocytes are phagocytic, the granular amebocytes exhibit NK-like activity, and the eleocytes contain chloragosomes which are used to secrete lytic substances (Cossarizza *et al*., 1995, 1996; Fuller-Espie *et al*., 2010). These celomocytes can be studied *in vitro* by experimentally inducing extrusion of the celomocyte rich celomic fluid through the dorsal pores. Once collected, these cells can be analyzed through flow cytometry where amebocytes (hyaline and granular) and eleocytes can be differentiated based on their size (forward scatter) and granularity (side scatter) (Cossarizza *et al*., 2005). Using flow cytometry, early apoptotic cells can be distinguished with DNA binding viability dyes such as propidium iodide (PI) and 7-aminoactinomycin D (7-AAD) that only penetrate late apoptotic and necrotic cells (Rabinovitch *et al*., 1986; Nicoletti *et al*., 1991). Additionally, changes in $\Delta\Psi$m and PS translocation can be detected through flow cytometry with the fluorescent compounds JC-1 and annexin V-FITC respectively (Salvioli *et al*., 1997; van Engeland *et al*., 1998; Fuller-Espie *et al*., 2010).

Materials and Methods

Cell culture supplies and chemical reagents

Tissue culture plasticware was purchased from Fisher Scientific. Phosphate buffered saline (PBS) was purchased from Invitrogen. Dulbecco's Modified Eagle Medium (DMEM, Invitrogen) was supplemented with Serum Supreme (Lonza BioWhittaker), plus 100µg ml^{-1} ampicillin (Shelton Scientific), 10µg ml^{-1} kanamycin (Shelton Scientific), 10µg ml^{-1} tetracycline, 5µg ml^{-1} chloramphenicol (Fluka Biochemika), 1×penicillin, streptomycin and amphotericin B (Invitrogen), 1×nonessential amino acids (Invitrogen), 1×L-glutamine (Invitrogen) and 1×HEPES (Invitrogen) to comprise Super DMEM (SDMEM). Copper (II) chloride ($CuCl_2$, 221783-100G) and cadmium chloride ($CdCl_2$, 655198-5G) were purchased from Sigma-Aldrich and stock solutions were prepared in deionized water and sterilized by filtration.

EW husbandry

Eisenia hortensis (European nightcrawlers) were purchased from Vermitechnology Unlimited, Orange Lake, Florida, USA, who imports *E. hortensis* from Star Food, Holland, Scherpenzeelseweg 95, 3772ME Barneveld, The Netherlands. Species identity was determined by the United States Department of Agriculture, USDA Permit #52262 (Vermitechnology, personal communication). Short-term colonies were maintained at RT in the dark on moistened autoclaved pine woodchips sprinkled with Single Grain Rice Cereal or Rice with Bananas Cereal (Gerber) and covered with autoclaved, shredded, and moistened paper towels. Habitats were changed twice weekly. Animals were euthanized by freezing at -20 ºC.

Extrusion of celomocytes

Prior to experimentation, EWs were first washed with distilled water on paper towels using a water bottle to remove wood chip fragments and food particles. They were then placed overnight on paper towels moistened with 2.5 µg ml^{-1} Fungizone (Fisher Scientific) in 100mm Petri dishes to minimize fecal contamination during the extrusion process, and remove further any surface contaminants. To collect celomocytes, EWs were placed in multichannel pipette reservoirs containing 3 ml BD FACSFlow sheath fluid (BD Biosciences). The EWs extruded their celomocytes through their dorsal pores in response to this external stimulus without the need to use the alcohol extrusion method reported by others (Engelmann *et al*., 2005). The celomocytes were then transferred to 0.5 ml Accumax (Innovative Cell Technology) in 15 ml conical test tubes for a 5 min incubation period at RT to reduce aggregation of cells. Finally, 6.5 ml PBS was added and the samples were centrifuged immediately at 150xg, 7 min at 4 ºC. After decanting the supernatant, the celomocyte pellet was gently mixed by flicking the bottom of the centrifuge tube, and celomocytes were resuspended in 1 ml SDMEM. Enumeration was carried out using a hemacytometer. Only large celomocytes (hyaline amebocytes) and small celomocytes (granular amebocytes) were included in the cell count; chloragocytes (eleocytes) were not counted but did factor into a quality score. Samples with large numbers of chloragocytes compared to large and small celomocytes were not used in assays due to their high background autofluorescence. Samples were adjusted to 1 x 10^6 celomocytes ml^{-1} in SDMEM.

EW coding

EWs were coded according to the particular *in vitro* assays in which their celomocytes were used. EWs used in detection of changes to $\Delta\Psi$m with JC-1 were labeled with a J and numbered (EW-J1 through EW-J20). EWs used in phosphatidylserine translocation and caspase assays detected with annexin V-FITC were labeled with AC and numbered (EW-AC1 through EW-AC10). Lastly, EWs used in the correlation assays were labeled with JA and numbered (EW-JA1 through EW-JA9).

$\Delta\Psi$m assays

Changes in $\Delta\Psi$m were measured with the lipophilic cationic fluorescent compound JC-1 (5,5',6,6'-tetrachloro-1,1',3,3'-tetraethylbenzimidazol-dazolcarbocyanine iodide) (Anaspec, 88060). JC-1 penetrates the plasma membrane readily entering the cytosol where it binds to intact mitochondrial membranes with large $\Delta\Psi$m and forms J-aggregates which emit orange at

590 nm when excited. During membrane depolarization these J-aggregates dissociate into the monomeric form which emit a green color at 527 nm (Salvioli *et al*., 1997). Using a BD FACSCalibur flow cytometer with a 488 nm excitation argon laser, celomocytes undergoing membrane depolarization were identified by increases in green fluorescence compared to the untreated control. 7-aminoactinomycin D (7-AAD) (BD Pharmingen, 559925) was also used to exclude dead cells from analyses.

Using a 96-well V-bottom plate, 1x 10^5 celomocytes in 0.1 ml SDMEM were added to experimental (cadmium and copper treated) and control [untreated (0 µM) double negative autofluorescent background; single positive JC-1; single negative JC-1, single positive 7-AAD] wells. Experimental wells received final concentration of 0 µM, 125 µM, 250 µM, or 500 µM of cadmium or copper, 5µg ml^{-1} JC-1, and 2.5 µl 7-AAD. Single positive JC-1 control wells received 20 µM valinomycin, single negative JC-1 control wells received 0 µM valinomycin, and single positive 7-AAD control wells received 0.01 % saponin (Acros 41923-1000). Experimental and control wells were incubated with medium, heavy metals, or valinomycin for 20 h at 25 ºC, 5 % CO_2. After incubation the cells were centrifuged at 150xg (5 min, 4 ºC) and washed once with 100 µl PBS. Cells in experimental wells were then resuspended in SDMEM containing JC-1 and 7-AAD; control wells were resuspended in SDMEM containing either JC-1 or 7-AAD/saponin. Cells were then incubated 15 min at RT in the dark, transferred to flow cytometry tubes on ice, and analyzed immediately by flow cytometry. The final outcome measure is based on the overall proportion of responder EWs to at least one of the concentrations of cadmium or copper employed.

Phosphatidylserine translocation and caspase assays

Translocation of phosphatidylserine (PS) from the plasma membrane inner leaflet to the outer leaflet was detected with fluorescein isothiocyanate (FITC)-conjugated annexin V (Invitrogen, ANNEXINV01). Upon translocation, PS is bound by the annexin V component and the FITC component emits at 518 nm detectable in the FL-1 channel. Similar to 7-AAD, propidium iodide (PI) (Invitrogen, P3566) also binds nucleic acids and was used to identify and exclude membrane-compromised cells of the late apoptotic and necrotic varieties. Upon excitation, PI emits at 617 nm which is detectable in the FL-2 channel.

The tripeptide caspase inhibitor *N*-benzyloxycarbonyl-Val-Ala-Asp-fluoromethyketone (Z-VAD-fmk) (BD Pharmingen, 550377), which binds to many caspases but principally inhibits caspases 1 and 3 (Yang *et al*., 2004), was used to test the involvement of caspase activity on PS translocation. Z-VAD-fmk enters the cell as an O-methyl ester and is converted to the active form within the cell by esterases (Shimizu and Pommier, 1997). Once active, the peptide irreversibly binds to and inhibits caspase function through its valine-alanine-aspartic acid (VAD) sequence. The aspartic acid at the P1 position of this peptide is specifically involved in this interaction where it alkylates the cysteine residue in the active site (Sarin, 1996). This peptide contains a fluoromethyl ketone (fmk) group responsible for anchoring to the caspase via a cysteine linkage and whose effects are controlled for with the dipeptide *N*-benzyloxycarbonyl-Phe-Ala-fluoromethylketone (Z-FA-fmk) (BD Pharmingen, 550411) which serves as a negative control (Braun *et al*., 1999). This peptide has a phenylalanine-alanine (FA) sequence which lacks the aspartic acid at the P1 position and therefore does not inhibit caspase activity in the cell.

Using a 96-well V-bottom plate, 1x10^5 celomocytes in 0.1ml SDMEM were added to experimental [cadmium-treated in 0.3 % DMSO (carrier control), cadmium- and Z-VAD-fmk-treated, and cadmium- and Z-FA-FMK-treated] and control [untreated (0 µM) double negative autofluorescent background; single positive annexin V-FITC; single positive PI] wells. Experimental wells received final concentrations of 0 µM, 62.5 µM, 125 µM, 250 µM, or 500 µM of cadmium, 40 µM Z-VAD-fmk or Z-FA-fmk, 2.5 µl annexin V-FITC, and 2.5 µl PI. Single positive annexin V-FITC control wells received 67.6 mM H_2O_2 (Fischer H325-500) and single positive PI control wells received 0.01 % saponin. Experimental and control wells were incubated with the cadmium and caspase inhibitor/negative caspase inhibitor control/DMSO carrier control for 20 h at 25 ºC, 5 % CO_2. After incubation the cells were centrifuged at 150x*g* (5 min, 4 ºC) and washed with 100 µl PBS. Cells in experimental wells were then resuspended in SDMEM, annexin V-FITC, and PI; control wells were resuspended in SDMEM and treated with either annexin V-FITC/H_2O_2 or PI/saponin to a final volume of 100 µl. Cells were then incubated 15 min at RT in the dark, transferred to flow cytometry tubes on ice and analyzed immediately by flow cytometry.

Correlation assays

The correlation between ongoing mitochondrial membrane depolarization and PS translocation was determined by conducting assays in which cells from individual EWs were assessed for both conditions independently. These assays were conducted simultaneously in separate V-bottom plates using the same protocols mentioned above without the addition of caspase inhibitors/negative inhibitor controls/DMSO carrier control. Experimental wells received final concentration of 0 µM, 50 µM, 250 µM, or 500 µM cadmium or copper.

Flow cytometry analysis

Fluorescence was measured using FL-1 (annexin V-FITC and JC-1), FL-2 (JC-1 and PI), and FL-3 (7-AAD) detectors of a FACSCalibur flow cytometer (BD Biosciences). Autofluorescent controls were used to set voltages for forward scatter (FSC), side scatter (SSC), FL-1, FL-2, and FL-3 during instrument set-up. Singly positive annexin V-FITC and PI controls were used to adjust compensation settings (spectral overlap removal) for PS assays and singly positive JC-1 and 7-AAD for $\Delta\Psi m$ assays. LISTMODE data was acquired and analyzed using Cell Quest Pro (BD Biosciences)

software. Only celomocytes corresponding to the large celomocytes (hyaline amebocytes) and small celomocyte (granular amebocytes) populations combined, as determined by appropriate size (FSC) (abscissa) and granularity (SSC) (ordinate), were gated for further analyses in region 1(R1) (Fig. 1A). Viable cells were only counted for analysis by gating on FL-2 (PI) or FL-3(7-AAD) negative events for PS and ΔΨm, respectively, in region 2(R2) (Fig. 1B). Changes in ΔΨm or PS were assessed by placing a marker (M1) on a FL-1 histogram gated on R1 and R2 at the median fluorescence value for untreated 0μM samples (Fig. 1D). This marker was set based on the untreated 0μM DMSO carrier control for analysis of PS translocation assays. Samples considered positive are those exhibiting a greater percentage of events occurring above the median fluorescence value measured in the untreated cells in the Fl-1 channel.

Statistical analysis

Data analysis and graphs were generated using Microsoft Excel 2007. The Student's t-test paired two samples for means was utilized with a 95 % confidence interval to determine if the experimental values were statistically significant as exhibited by a p-value less than or equal to 0.05. Only events exhibiting statistically significant increases above background are reported for ΔΨm and correlation assays; only events exhibiting statistically significant decreases in Z-VAD-FMK treated groups compared to Z-FA-FMK treated groups are counted as positive events for PS caspase assays. Linear correlation between ΔΨm and PS was determined by calculating Pearson product-moment correlation coefficients (*r*). Degree of correlation was dependent by the magnitude of positive *r*-values with values from 0.5 to 1.0 considered strong correlations. All data is based on averages of triplicate samples except EW-J1 and EW-J2 which were performed in duplicate.

Results

Flow cytometric detection of changes in ΔΨm

Early apoptotic celomocytes were identified with the viability dye 7-aminoactinomycin D (7-AAD) which only penetrates membrane-compromised cells and binds to nucleic acids. Upon excitation, membrane-compromised cells, such as those that are late apoptotic and necrotic, will emit at 650 nm which is detectable in the FL-3 channel (Rabinovitch *et al*., 1986). Using three-color analysis, these events were excluded so that only live and early apoptotic celomocytes could be evaluated for changes in ΔΨm. Figure 1 illustrates how data was collected and analyzed to detect alterations in ΔΨm in response to varying concentrations of cadmium and copper. Shown in Fig. 1D is the typical profile observed for the untreated negative control (left), valinomycin-treated positive control (middle), and heavy metal-treated sample (right).

Twenty-nine EWs in total were assayed for alterations in ΔΨm at cadmium or copper concentrations of 50 μM, 125 μM, 250 μM, and 500 μM as summarized in Table 1 where 6 EWs were assessed at 50 μM, 5 EWs at 125 μM, 8 EWs at 250 μM, and 27 EWs at 500 μM of cadmium or copper. Response rates for cadmium were varied but were recorded above the 50 % marker region for all concentrations other than 125 μM with a total response of 58.7 % for all EWs at all concentrations. Responses for copper were generally lower with a maximum response of 50 % for 250 μM. Total response for copper among all EWs for all concentrations was lower than cadmium at only 37 %.

Table 2 Caspase involvement for PS translocation in response to cadmium exposure

PS	Cd62.5	Cd125	Cd250	Cd500
EW-AC1	-	-	T	T
EW-AC2	-	-	T*	T
EW-AC3	-	-	T	T
EW-AC4	-	-	T*	T
EW-AC5	-	-	T*	T
EW-AC6	T	T*	-	-
EW-AC7	T	T*	-	-
EW-AC8	T	T	-	-
EW-AC9	T	T*	-	-
EW-AC10	T	T	-	-
% Response	**0% (0/5)**	**60% (3/5)**	**60% (3/5)**	**0% (0/5)**

EWs were treated at cadmium concentrations of 62.5 μM, 125 μM, 250 μM, and 500 μM. Statistically significant decreases ($p \leq 0.05$) in Z-VAD-fmk treated celomocytes compared to the Z-FA-fmk negative caspase control were exhibited only at concentrations of 125 μM and 250 μM in 60 % of EWs. - = not tested, T = tested, T* = tested and statistically significant.

Interference of phosphatidylserine translocation with caspase inhibitors

Flow cytometric data was collected and analyzed similarly to ΔΨm shown in Fig. 1. Ten EWs in total were assayed for inhibition of cadmium-induced PS translocation: five (EW-AC1-5) at concentrations of 62.5 μM and 125 μM, and another five (EW-AC6-10) at the higher concentrations of 250 μM and 500 μM (Table 2). Representative data for 2 EWs (EW-AC6 and EW-AC7) at 125μM is shown in Fig. 2 where cadmium treatment with DMSO and Z-FA-fmk produced significant increases compared to untreated samples and cadmium treated Z-VAD-fmk samples were inhibited compared to untreated samples. When treated at concentrations of 125 μM and 250 μM, significant inhibition of PS translocation was observed in 60 % of cases compared to the Z-FA-fmk negative control, but was not observed at the lowest (62.5 μM)

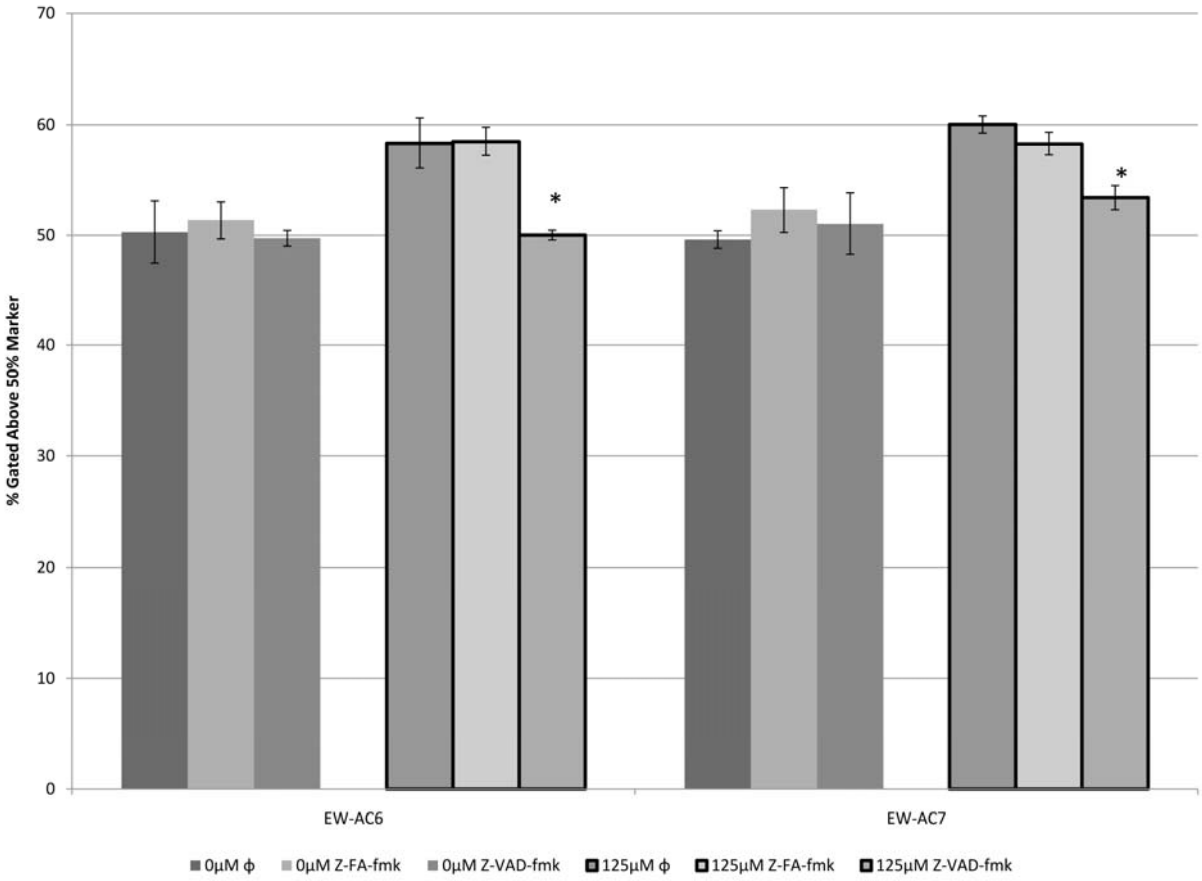

Fig. 2 Representative interference of PS translocation using caspase inhibitor. The percent viable hyaline and granular amebocytes exhibiting PS translocation above the 50 % M1 marker for each treatment is shown for two EWs (EW-AC6 and EW-AC7). For each EW the left set of bars is the untreated 0 μM cadmium control and the right set of bars with borders is 125 μM cadmium treated. For each set the first bar is the DMSO carrier control, the second is treated with the negative control of caspase inhibition (Z-FA-fmk), and the third is treated with the general caspase inhibitor Z-VAD-fmk. Statistically significant decreases (*, $p \leq 0.05$) compared to the negative caspase control are shown for both EWs at 125 μM. Error bars indicate standard deviation.

or highest (500 μM) concentrations as summarized in Table 2.

Correlation of changes in ΔΨm and phosphatidylserine translocation

Since mitochondrial membrane depolarization and PS translocation are both hallmarks of early apoptosis, there was an interest in the existence of correlation between these two events. These separate events were evaluated for nine EWs in two separate assays: one using copper and cadmium concentrations of 250 μM and 500 μM for a two-fold difference, and another using 50 μM and 500 μM for a ten-fold difference (Fig. 3). These events were detected to some degree at all concentrations used except ΔΨm at a copper concentration of 50 μM (Table 3). A very high degree of correlation was found with eight EWs correlating strongly and mean *r* value of 0.71. Results for EWs EW-JA7 through EW-JA9 are shown in Fig. 3. Note the strong correlation between events and concentrations for EW-JA7 where there is a decreasing effect moving from 500 μM to 50 μM and from cadmium to copper. The only EW that did not correlate strongly was EW-JA9 where at 500 μM copper PS translocation increased but ΔΨm decreased.

Discussion

This study demonstrates that the heavy metals cadmium (50 - 500 μM) and copper (125-500 μM) induce the early apoptotic event of mitochondrial membrane depolarization in celomocytes of the EW *E. hortensis.* It was found that cadmium induced an equal, if not greater, response at every concentration measured with a total response rate of 58.7 % compared to copper at 37 %. Copper required a higher concentration than cadmium (125 μM vs. 50 μM) to induce membrane depolarization. The decrease of membrane potential has also been reported for both metals in rat hepatocytes and for cadmium in human intestinal cells (Martel *et al*., 1990; Pourahmad, 2000; Bolduc *et al*., 2004). Pourahmad (2000) also reported a similar effect where cadmium induced depolarization at lower concentrations than copper (20 vs. 50 μM). Although

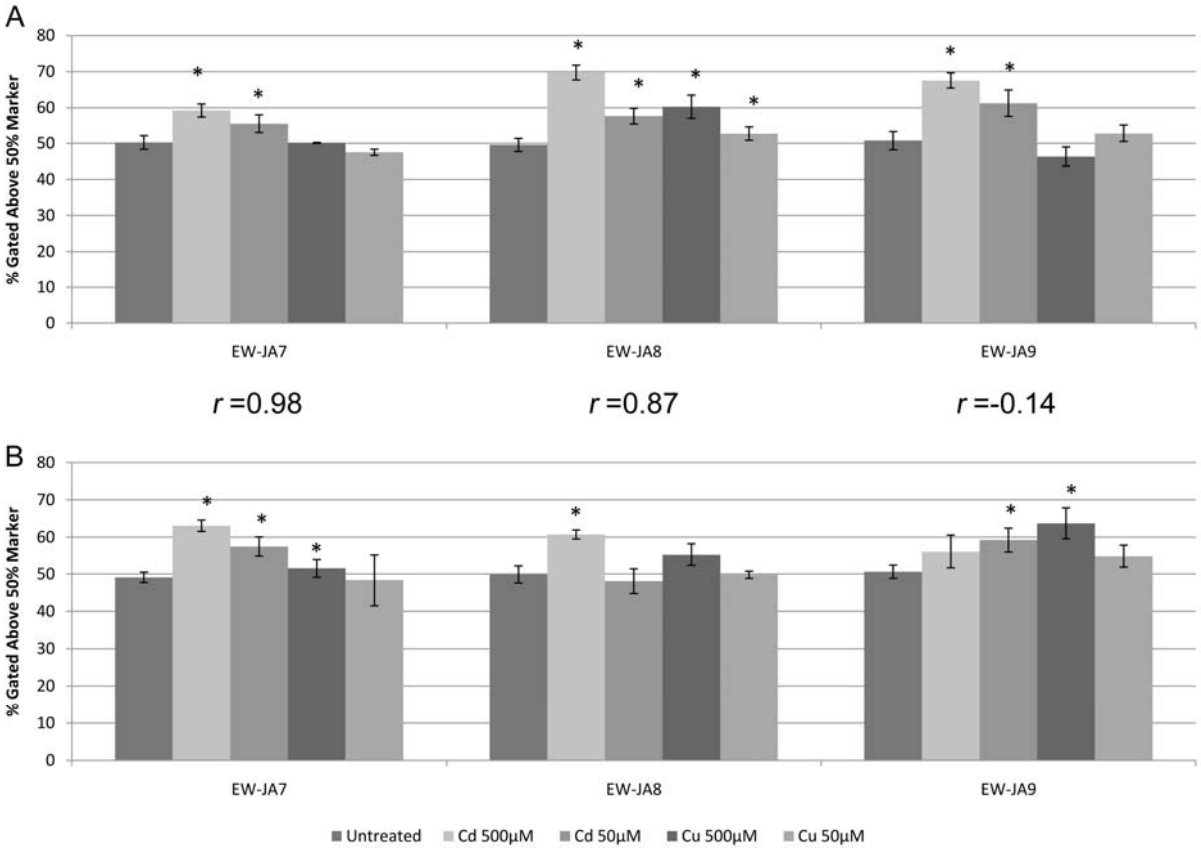

Fig. 3 Loss of ΔΨm and PS translocation are correlated. In the assay using 50 µM and 500 µM $CdCl_2$, the percent viable hyaline and granular amoebocytes exhibiting loss of ΔΨm (A) and PS translocation (B) above the 50 % M1 marker for each treatment is shown for 3 EWs. Statistically significant increases (*, $p \leq 0.05$) compared to the untreated control are indicated. The correlation coefficient (*r)* is indicated for each EW where EW-JA7 and EW-JA8 are strongly correlated whereas EW-JA9 is not. Error bars indicate standard deviation.

concentrations needed for a response in celomocytes of *E. hortensis* were higher than those needed in rat hepatocytes, EW cells may be adapted to higher concentrations since they bioaccumulate these metals from the naturally metalliferous soils they live in (Morgan and Morgan, 1988). This tolerance may be attributed to heavy metal binding proteins such as those for cadmium demonstrated in *Eisenia foetida* and copper in the annelid *Eudistylia vancouveri* (Young and Roesijadi, 1983; Suzuki *et al*, 1980). It would be interesting to investigate the presence of similar proteins in our *E. hortensis* model to confirm this.

Additionally, the caspase dependence of cadmium on PS translocation was also investigated. In regards to the events of early apoptosis, mitochondrial membrane depolarization is one of the earliest apoptotic events with caspase independent pathways and typically precedes PS translocation (Bortner and Cidlowski, 1999; Fabbri *et al*., 2006). Translocation of PS has been shown to be dependent upon caspase-3 which is inhibited by Z-VAD-fmk (Marianski *et al*., 2002). Little is known of caspase involvement in EWs although exogenous H_2O_2 has been shown to activate caspases in the *E. hortensis* model (Fuller-Espie *et al*., 2010). Results of this study show that caspases also play a role in the translocation of PS induced by cadmium in celomocytes of *E. hortensis* as measured with annexin V-FITC. It was shown that caspase involvement only occurred within a narrow range of 125-250 µM. It is possible that Z-VAD-fmk is not active at concentrations lower than this since low doses of cadmium (5-20 µM) have been shown to have inhibitory effects as well (Yuan *et al*., 2000). At the higher concentration it is possible that cadmium is subverting caspase dependent pathways through oxidative induction of PS translocation and is therefore unaffected by Z-VAD as has been shown in human lung cells (Shih *et al*., 2003). It would be interesting to study these oxidative effects in parallel to PS translocation with a fluorescent detector of ROS such as dihydrorhodamine123 or dihydroethidium (Kagan *et al*., 2002; Fuller-Espie *et al*., 2010).

Lastly, the relation between mitochondrial membrane depolarization and PS translocation was also investigated in celomocytes of *E. hortensis* exposed to cadmium and copper. It was found that these events correlated strongly ($r > 0.5$) in 89 % of

Table 3 Correlation between loss of ΔΨm and PS translocation

$\Delta\Psi_m$ and PS	Cd50		Cd250		Cd500		Cu50		Cu250		Cu500		*r*	Correlation
	ΔΨm	PS	ΔΨm	PS	ΔΨm	PS	ΔΨm	PS	ΔΨm	PS	ΔΨm	PS		
EW-JA1	-	-	T*	T*	T*	T*	-	-	T*	T*	T*	T*	0.80	Strong
EW-JA2	-	-	T	T*	T	T*	-	-	T*	T*	T*	T*	0.69	Strong
EW-JA3	-	-	T	T	T*	T*	-	-	T*	T*	T*	T*	0.84	Strong
EW-JA4	T*	T*	-	-	T*	T*	T	T	-	-	T*	T*	0.69	Strong
EW-JA5	T	T	-	-	T*	T*	T	T	-	-	T*	T*	0.71	Strong
EW-JA6	T	T	-	-	T*	T*	T	T	-	-	T*	T*	0.97	Strong
EW-JA7	T*	T*	-	-	T*	T*	T	T	-	-	T*	T	0.98	Strong
EW-JA8	T	T*	-	-	T*	T*	T	T*	-	-	T	T*	0.87	Strong
EW-JA9	T*	T*	-	-	T	T*	T	T	-	-	T*	T	-0.14	None
% Response	**50%** (3/6)	**67%** (4/6)	**33%** (1/3)	**67%** (2/3)	**78%** (7/9)	**100%** (9/9)	**0%** (0/6)	**17%** (1/6)	**100%** (3/3)	**100%** (3/3)	**89%** (8/9)	**78%** (7/9)	**Mean 0.71**	**89%** (8/9)

EWs were treated in two separate assays at cadmium and copper concentrations of 50 µM and 500 µM for a ten-fold difference, or 250 µM and 500 µM for a two-fold difference. Loss of ΔΨm and PS translocation were strongly correlated ($r > 0.5$) in 89 % of cases with an average *r* value of 0.71. Statistically significant increases ($p \leq 0.05$) were present for both events and both heavy metals. - = not tested, T = tested, T* = tested and statistically significant.

cases (8 of 9 EWs) with an average *r* value of 0.71. These data suggest that loss of membrane potential is not a pre-requisite for externalization of PS since in many cases PS translocation was detected while depolarization of the mitochondrial membrane was not such as in EW-JA2 for cadmium at 250 µM and 500 µM. The use of an inhibitor of mitochondrial membrane depolarization and cytochrome c release like ursodeoxycholic acid would help determine the involvement of loss of ΔΨm on PS translocation (Rodrigues *et al*., 1999). These data also show that heavy metal toxicity is inducing these early apoptotic events after the same exposure time (20 h) which could further be studied to determine if exposure time is associated with apoptosis induction such as 9-14 h for cadmium as shown in mouse liver (Habeebu *et al*., 1998).

Acknowledgments

This work was funded by the Pennsylvania Academy of Science and the Cabrini College Science Department Research Fund.

References

An Y. Soil ecotoxicity assessment using cadmium sensitive plants. Environ. Pollut. 127: 21-26, 2004.

Arnold R, Hodson M, Black S, Davies N. The influence of mineral solubility and soil solution concentration on the toxicity of copper to *Eisenia fetida* Savigny. Pedobiologia 47*:* 622-632, 2004.

Belyaeva E, Dymkowska D, Wieckowski M, Wojtczak L. Mitochondria as an important target in heavy metal toxicity in rat hepatoma AS-30D cells. Toxicol. Appl. Pharmacol. 231: 34-42, 2008.

Blanco G, Bustamante J, Garcia M, Hajos S. Hydrogen peroxide induces apoptotic-like cell death in coelomocytes of *Themiste petricola* (Sipuncula). Biol. Bull. 209: 168-83, 2005.

Bolduc JS, Denizeau F, Jumarie C. Cadmium-induced mitochondrial membrane-potential dissipation does not necessarily require cytosolic oxidative stress: studies using rhodamine-123 fluorescence unquenching. Toxicol. Sci. 77: 299-306, 2004.

Bortner CD, Cidlowski JA. Caspase independent/dependent regulation of K(+), cell shrinkage, and mitochondrial membrane potential during lymphocyte apoptosis. J. Biol. Chem. 274: 21953-62, 1999.

Braun J, Novak R, Herzog K, Bodner S, Cleveland J, Tuomanen E. Neuroprotection by a caspase inhibitor in acute bacterial meningitis. Nat. Med. 5: 298-302, 1999.

Collazo C, Chacón O. Programmed cell death in plants resembles apoptosis of animals. Biotecnología Aplicada 23, 1-10, 2006.

Cossarizza A, Cooper E, Quaglino D, Salvioli S, Kalachnikova G, Franceschi C. Mitochondrial mass and membrane potential in coelomocytes from the earthworm *Eisenia foetida*: studies with fluorescent probes in single intact cells. Biochem. Biophys. Res. Commun. 214: 503-510, 1995.

Cossarizza A, Cooper E, Suzuki M, Salvioli S, Capri M, Gri G, *et al*. Earthworm leukocytes that are not phagocytic and cross-react with several

human epitopes can kill human tumor cell lines. Exp. Cell Res. 224: 174-82, 1996.
Cossarizza A, Pinti M, Troiano L, Cooper E. Flow cytometry as a tool for analysing invertebrate cells. Inv. Surv. J. 2: 32-40, 2005.
Engelmann P, Palinkas L, Cooper EL, Németh P. Monoclonal antibodies identify annelid four distinct leukocyte markers. Dev. Comp. Immunol. 29: 599-614, 2005.
Fabbri F, Carloni S, Brigliadori G, Zoli W, Lapalombella R, Marini M. Sequential events of apoptosis involving docetaxel, a microtubule-interfering agent: a cytometric study. BMC Cell Biol. 7:6, 2006.
Fadeel B, Xue D. The ins and outs of phospholipid asymmetry in the plasma membrane: roles in health and disease. Crit. Rev. Biochem. Mol. Biol. 44: 264-77, 2009.
Fesik S, Shi Y. Controlling the caspases. Science 294: 1477-8, 2001.
Fuller-Espie SL, Nacarelli T, Blake E, Bearoff, FM. The effect of oxidative stress on phagocytosis and apoptosis in the earthworm *Eisenia hortensis*. Inv. Surv. J. 7: 89-106, 2010.
Haanen C, Vermes I. Apoptosis : Programmed cell death in fetal development. Eur. J. Obstet. Gynecol. Reprod. Biol. 64: 129-133, 1996.
Habeebu S, Liu J, Klaassen C. Cadmium-induced apoptosis in mouse liver. Toxicol. Appl. Pharmacol. 149: 7, 1998.
Harrison L, Brown C, Afonso C, Zhang J, Susta L. Early occurrence of apoptosis in lymphoid tissues from chickens infected with strains of Newcastle disease virus of varying virulence. J. Comp. Pathol. 2011.
Hartenstein V. Blood cells and blood cell development in the animal kingdom. Annu. Rev. Cell. Dev. Biol. 22: 677-712, 2006.
Hirano T, Tamae K. Heavy metal-induced oxidative DNA damage in earthworms: a review. Appl. Environ. Soil Sci. 2010: 1-7, 2010.
Kagan V, Fabisiak J, Shvedova A, Tyurina Y, Tyurin V, Schor N, *et al*. Oxidative signaling pathway for externalization of plasma membrane phosphatidylserine during apoptosis. FEBS Lett. 477: 1-7, 2000.
Kagan V, Gleiss B, Tyurina Y, Tyurin VI, Elenstrom-Magnusson C, Liu S, *et al*. A role for oxidative stress in apoptosis: Oxidation and externalization of phosphatidylserine is required for macrophage clearance of cells undergoing Fas-mediated apoptosis. J. Immunol. 169: 487-499, 2002.
Kim S, Jeong H, Myung N, Kim M, Lee J, So H, *et al*. The protective mechanism of antioxidants in cadmium-induced ototoxicity in vitro and in vivo. Environ. Health Perspect. 116: 854-62, 2008.
Kinchen J. A model to die for: signaling to apoptotic cell removal in worm, fly and mouse. Apoptosis 15*:* 998-1006, 2010.
Kiss T. Apoptosis and its functional significance in molluscs. Apoptosis 15: 313-21, 2010.
Lewis K. Programmed death in bacteria. Mol. Biol. Rev. 64: 503-514, 2000.
Ly J, Grubb D, Lawen A. The mitochondrial membrane potential ($\Delta\Psi_m$) in apoptosis; an update. Apoptosis 8*:* 115-28, 2003.
Mandal D, Moitra P, Saha S, Basu J. Caspase 3 regulates phosphatidylserine externalization and phagocytosis of oxidatively stressed erythrocytes. FEBS Lett. 513: 184-8, 2002.
Marianski NA, Frederik P, Mul JD, vanBuul DR, Kuijpers TW. Granulocyte colony-stimulating factor inhibits the mitochondria-dependent activation of caspase-3 in neutrophils. Blood 99: 62-679, 2002.
Martel J, Marion M, Denizeau F. Effect of cadmium on membrane potential in isolated rat hepatocytes. Toxicology 60: 161-172, 1990.
Martin J, Mahlke K, Pfanner N. Role of an energized inner membrane in mitochondrial protein import. Delta psi drives the movement of presequences. J. Biol. Chem. 266: 18051-7, 1991.
Morgan J, Morgan A. Earthworms as biological monitors of cadmium, copper, lead and zinc in metalliferous soils. Environ. Pollut. 54: 123-138, 1988.
Mulder C, Baerselman R, Posthuma L. Empirical maximum lifespan of earthworms is twice that of mice. Age (Dordr) 29: 229-31, 2007.
Nicoletti I, Migliorati G, Pagliacci M, Grignani F, Riccardi C. A rapid and simple method for measuring thymocyte apoptosis by propidium iodide staining and flow cytometry. J. Immunol. Meth. 139*:* 271-279, 1991.
Pourahmad J. A comparison of hepatocyte cytotoxic mechanisms for Cu2+ and Cd2+. Toxicology 143: 263-273, 2000.
Rabinovitch P, Torres R, Engel D. Simultaneous cell cycle analysis and two-color surface immunofluorescence using 7-amino-actinomycin D and single laser excitation: applications to study of cell activation and the cell cycle of murine Ly-1 B cells. J. Immunol. 136: 2769-75, 1986.
Rodrigues C, Ma X, Linehan-Stieers C, Fan G, Kren B, Steer C. Ursodeoxycholic acid prevents cytochrome c release in apoptosis by inhibiting mitochondrial membrane depolarization and channel formation. Cell Death Differ. 6: 842-54, 1999.
Salvioli S, Ardizzoni A, Franceschi C, Cossarizza A. JC-1, but not DiOC6(3) or rhodamine 123, is a reliable fluorescent probe to assess delta psi changes in intact cells: implications for studies on mitochondrial functionality during apoptosis. FEBS Lett. 411: 77-82, 1997.
Sarin A. Different interleukin-1beta converting enzyme (ICE) family protease requirements for the apoptotic death of T lymphocytes triggered by diverse stimuli. J Exp Med 184: 2445-2450, 1996.
Shih C, Wu J, Ko W, Wang L, Wei Y, Liang H, *et al*. Mitochondria-mediated caspase-independent apoptosis induced by cadmium in normal human lung cells. J. Cell Biochem. 89: 335-47, 2003.
Shimizu T, Pommier Y. Camptothecin-induced apoptosis in p53-null human leukemia HL60 cells and their isolated nuclei: effects of the protease inhibitors Z-VAD-fmk and dichloroisocoumarin suggest an involvement of both caspases and serine proteases. Leukemia 11*:* 1238-1244, 1997.

Suzuki K, Yamamura M, Mori T. Cadmium-binding proteins induced in the earthworm. Arch. Environ. Contam. Toxicol. 9: 415-424, 1980.

van Engeland M, Nieland L, Ramaekers F, Schutte B, Reutelingsperger C. Annexin V-affinity assay: a review on an apoptosis detection system based on phosphatidylserine exposure. Cytometry 31: 1-9, 1998.

Yang B, El Nahas A, Fisher M, Wagner B, Huang L, Storie I, *et al*. Inhibitors directed towards caspase-1 and -3 are less effective than pan caspase inhibition in preventing renal proximal tubular cell apoptosis. Nephron Exp. Nephrol. 96: 39-51, 2004.

Young J, Roesijadi G. Reparatory adaptation to copper-induced injury and occurrence of a copper-binding protein in the polychaete, *Eudistylia vancouveri*. Mar. Pollut. Bull. 14: 30-32,1983.

Yuan C, Kadiiska M, Achanzar W, Mason R, Waalkes M. Possible role of caspase-3 inhibition in cadmium-induced blockage of apoptosis. Toxicol. Appl. Pharmacol. 164: 321-9, 2000.